INTERNATIONAL JOURNAL OF OPTIMIZATION IN CIVIL ENGINEERING
Int. J. Optim. Civil Eng., 2022; 12(4): 595-608

ROBUST DESIGN OPTIMIZATION OF SPACE TRUSS STRUCTURES

P. Hosseini[1], A. Kaveh[2*, †] and S. R. Hoseini Vaez[3]
[1]*Faculty of Engineering, Mahallat Institute of Higher Education, Mahallat, Iran*
[2]*School of Civil Engineering, Iran University of Science and Technology, Tehran-16, Iran*
[3]*Department of Civil Engineering, Faculty of Engineering, University of Qom, Qom, Iran*

ABSTRACT

The existence of uncertainties in engineering problems makes it essential to consider these effects at all times. Robust design optimization allows a design to be made less sensitive to uncertain input parameters. Actually, robust design optimization reduces the sensitivity of the objective function and the variations in design performance when uncertainty exists. In this study, two space trusses were optimized based on the modulus of elasticity, yield stress, and cross-sectional uncertainties in order to increase the response robustness and decrease the weight. The displacement of one node has been used as the criterion for Robust Design Optimization (RDO) of these two structures. Two trusses with 72 members and 582 members are considered, which are famous trusses in the field of structural optimization. Also, the EVPS meta-heuristic algorithm was employed which is an enhanced version of the VPS algorithm based on the single degrees of freedom of a system with viscous damping.

Keywords: robustness index; enhanced vibrating particles system algorithm; size optimization; truss structures; robustness design optimization.

Received: 15 June 2022; Accepted: 20 August 2022

1. INTRODUCTION

A key application of optimization in knowledge engineering is optimal design. By using this design, engineering problems can be solved by making proper use of what is limited. Although metaheuristic algorithms are frequently used to optimize problems in a reasonable amount of time, these methods do not guarantee that the best answer will be obtained. As a

[*]Corresponding author: School of Civil Engineering, Iran University of Science and Technology, Tehran-16, Iran
[†]E-mail address: alikaveh@iust.ac.ir (A. Kaveh)

result of structural optimization, economical designs can be achieved, and it is an active topic in the field of civil, particularly structural engineering. Structural optimization is heavily reliant on meta-heuristic algorithms, such as the following:

Particle Swarm Optimization (PSO) [1], Differential evolution algorithm (DE) [2], League championship algorithm [3], Search and rescue optimization algorithm (SAR) [4], Teaching–learning-based optimization [5], Grey wolf optimizer [6], Simplified dolphin echolocation algorithm (SDE) [7-9], water wave optimization (WWO) [10], Honey Badger Algorithm [11].

The evaluation of the structure's reliability is an interesting problem in structure optimization. In probability theory, reliability theory links system performance to what is expected of it in practice. Several design parameters, such as material properties, geometric dimensions, and external loads, are subject to uncertainty in engineering problems. As a result, the presence of uncertainty can have a significant impact on structural safety, which necessitates a method for assessing reliability. To guarantee averting failure, a safety coefficient can be applied to address uncertainty. The following studies have examined the effects of structural uncertainty during the evaluation of the structural:

For the purpose of determining optimal solutions for uncertain convex optimization problems, Calafiore and Dabbene considered two standard philosophies [12]. Based on the classical stochastic optimization methodology, the optimal design was aimed at minimising the expected values of the objective function under uncertainty (average approach), whereas in the second approach, it is intended to minimize the worst-case objective (worst-case or min–max approach).

Asadpoure et al presented examples of truss structures to illustrate the importance of incorporating the control of variability into the design process [13]. Additionally, results obtained from the proposed method were in excellent agreement with those obtained from a Monte Carlo optimization algorithm.

A robust design optimization of truss structures with uncertain-but-bounded parameters and loads was investigated by Kang and Bai [14]. A non-probabilistic ellipsoid convex model was used to treat variations in cross-sectional areas, Young's moduli, and applied loads. Using a robustness index to quantify the maximum allowable magnitude of system variations, a design problem was formulated to maximize the minimum of the robustness indices under a given material volume constraint for all the concerned design requirements.

Richardson et al presented an approach to robust topology optimization for truss structures with uncertain materials and loads, as well as discrete design variables [15]. As part of the problem formulation, uncertainties regarding the load and spatially correlated material stiffness are considered, as well as the length of truss elements. In comparison to classical scalar random variable approaches, a more realistic random field representation of material uncertainty was achieved.

A multi-objective genetic programming approach was presented by Assimi et al. in 2019 for the optimization of truss sizing and topology [16]. To achieve a tradeoff solution that will satisfy all the optimization objectives functions subject to constraints such as kinematic stability, maximum allowable stress in members, and nodal deflections, it aims to determine the optimal cross-sectional areas and connectivities between the nodes. Furthermore, it utilized computer programs to represent potential solutions before evolving to a final set of options.

Kaveh et al investigated the effect of the Modified Dolphin Monitoring (MDM) operator on three well-known steel frame structures based on the Hasofer-Lind method [17]. EVPS and VPS algorithms were used to calculate the reliability index, as well as the MDM operator applied to them and the last story drift as a limit state function.

Hoseini Vaez et al. examined the reliability of truss structures in the context of natural frequency constraints in 2020 [18]. By using the Hasofer-Lind method and meta-heuristic algorithms, they calculated the reliability index based on the frequency of the first mode and the objective function of the problem.

A reliability-based optimal design of two dome truss structures considering the probability of frequency was developed by Hoseini Vaez et al. [19]. Using Monte Carlo simulation, the reliability index was calculated and two metaheuristic algorithms were used to optimize the process

Using meta-heuristic algorithms and the Monte Carlo method, Hosseini et al. developed an optimal design for transmission line towers based on reliability in 2020 [20]. A limit state function was defined using node displacement, nodal loads, and modulus of elasticity as random variables.

A study by Hoseini Vaez et al in 2022 evaluated the safety probability of two two-dimensional steel moment-resisting frames and examined the effect of uncertainties on each design parameter on the maximum frame drift [21]. Additionally, energy dissipated in the stories of the frames was evaluated with respect to its robustness index. Random variables were distributed with a normal probability distribution to model the uncertainties.

This study examined the robust design optimization of two steel trusses taking into account the uncertainties associated with their modulus of elasticity, yield stress, and cross-sections. It is considered that parameters with uncertainty are random variables, each of which has a statistical distribution. There is actually a normal probability distribution of random variables used to model the uncertainties. The structural analysis was conducted using finite element analysis.

In this article, the objective is to design truss structures that are as lightweight as possible and have the lowest robustness index possible. This research utilized the EVPS meta-heuristic algorithm, which is a structural optimization algorithm. Several studies have already used similar algorithms to solve structural optimization problems [22-29].

The paper is organized as follows: The introduction is presented in the first section. In section 2, an enhanced vibrating particles system (EVPS) algorithm is briefly discussed. Section 3 contains the formulation of the objective function. The fourth section of the paper examines two benchmark problems using the EVPS algorithm. In the last section, the conclusion is presented.

2. THE EVPS ALGORITHM

This algorithm is an enhanced version of the VPS algorithm, which is based on free vibration of freedom systems' single degrees with viscous damping. As a result of the improvement, the convergence speed is increased, the search capability is enhanced, the EVPS is able to escape from local optima, and the result is an improved inference [30]. The *Memory* parameter of the EVPS algorithm has been replaced with the *HB* parameter of the

VPS algorithm. *Memorysize* is the number of the best historically positioned positions from the whole population saved by the *Memory* parameter. If the best answer of each iteration is better than the worst value in the *Memory*, it should be replaced by the best answer. In addition, the equations for generating the population for the next iteration have been changed in the EVPS algorithm.

3. ROBUST DESIGN FORMULATION

As well as satisfying specific design constraints, the goal is to minimize the weight of structures and the robustness index. According to the LRFD-AISC specification [30], these constraints include strength and displacement constraints. In mathematical terms, the formulation is as follows:

$$\begin{aligned} &\text{Find } \{x\} = [x_1, x_2, ..., x_{ng}] \quad x_i \in S_i \\ &\text{To minimize } \begin{cases} W(\{\mathrm{x}\}) = \sum_{i=1}^{nm} \rho_i A_i L_i \\ \textit{Robustness index}(\{\mathrm{x}\}) \end{cases} \\ &\text{Subjected to } \begin{cases} g_j(\{\mathrm{x}\}) \le 0, \quad \mathrm{j} = 1, 2, ..., \mathrm{nc} \\ \mathrm{x}_{i_{\min}} \le x_i \le \mathrm{x}_{i_{\max}} \end{cases} \end{aligned} \tag{1}$$

where *{x}* is a set of design variables containing the cross sectional area; *ng* is the number of member groups (number of design variables); *W({x})* is the structure's weight; *nm* is the number of elements; *nc* is the number of constraints; ρ_i represents the density of material in the structure; A_i and L_i indicate the cross-sectional area and length of member *i*, respectively. The objective of Eq. (1) is not only to obtain the least weight but also to achieve the minimum robustness index of a specified node in three directions. The minimum robustness index*({x})* represents the Monte Carlo model of optimal answers with the least standard deviation.

There have been many studies on the topic of robustness. Different methods have been proposed so far under different issues [31-32]. Robust responses should minimize the effect of probabilistic variables on the final result and the dispersion of the response. To measure dispersion, the normalized standard deviation has been selected as the robustness index.

According to Eq. (2), the objective is to estimate Eq. (1) as follows:

$$\textit{Objective function} = \alpha \frac{WS\{x\}}{AOW} + \beta \frac{SDS\{x\}}{AOSD} \tag{2}$$

where WS{x} and AOW are the Structure Weight (WS) of the xth design variable and the Optimized Weight (AOW) without taking the robustness index into account, SDS{x} and AOSD are the Standard Deviation of Structures (SDS) of the xth design variable and an

Optimized Standard Deviation (AOSD) without taking into account weight. The present study examined the robustness index of the displacement of a specified node in three directions.also α and β represent the effect of the structure's weight and robustness index, respectively.

According to Eq. (2), the objective of this study is to minimize both weight and robustness index simultaneously while satisfying the constraints of the problem.

4. NUMERICAL PROBLEMS

To investigate the performance of the EVPS algorithm, two benchmark problems are presented. It is noted that the values of the population size for the first problem, the population size for the second problem, the total number of iterations, p, w1, w2, HMCR, PAR, and Memorysize are 40, 70, 300, 0.2, 0.3, 0.3, 0.95, 0.1, and 4, respectively. All problems are subjected to thirty independent optimization runs. For the analysis of the two trusses, Monte Carlo simulation was used with 10^5 random samples, and modulus of elasticity, yield stress, and cross-sections were taken as random variables with 5% coefficients of variation.4.1 A 72-bar spatial truss.

4.1 A 72-bar spatial truss

FIg. 1 illustrates a 72-bar spatial truss structure. There are 16 design groups based on the elements:
(1) A1_A4, (2) A5_A12, (3) A13_A16, (4) A17_A18, (5) A19_A22, (6) A23_A30, (7) A31_A34, (8) A35_A36, (9) A37_A40, (10) A41_A48, (11) A49_A52, (12) A53_A54, (13) A55_A58, (14) A59_A66 (15), A67_A70, and (16) A71_A72.

It is assumed that the material density is 0.1 lb/in^3 and the modulus of elasticity is 10,000 ksi. Stress limits are set at ±25 ksi for the members. Nodes are subject to displacement limits of ±0.25 inches. Members are permitted to have a minimum cross-sectional area of 0.10 in^2 and a maximum cross-sectional area of 4.00 in^2. The loading conditions are as follows:

LC1. At node 1: 5, 5 and -5 kips are loaded in the x, y, and z directions, respectively.

LC2. There is a load -5 kips in the z direction at nodes 1, 2, 3 and 4.

Table 1 presents the results for the optimal design obtained by using the weight part of Eq. (1) along with the effect of both parts of Eq. (1). Additionally, the results are compared with the different coefficients of α and β. According to Table 1, with an increase in the β coefficient, the weight of the structure and the robustness index will increase. According to Eq. (3), the objective function is considered in this example based on the conditions of the problem.

$$Objective\ function = \alpha \frac{WS\{x\}}{379.64} + \frac{\beta}{3}\left[\frac{SDS_x\{x\}}{0.0022} + \frac{SDS_y\{x\}}{0.0022} + \frac{SDS_z\{x\}}{0.00041}\right] \tag{3}$$

where, according to the first loading, SDS_x, SDS_y and SDS_z correspond to the displacement of node 1 in the x, y, and z directions, since this is the most critical loading for the displacement of nodes.

Based on different values of α and β, FIg. 2 illustrates the convergence curves for the 72-

bar spatial truss. As shown in FIg. 3, the absolute stress limitation obtained using the EVPS algorithm for different α and β for the 72-bar spatial truss is compared, while FIg. 4 illustrates a comparison of the displacement limitations in 3 directions obtained by using the EVPS algorithm for different types of α and β for the 72-bar spatial truss for LC1.

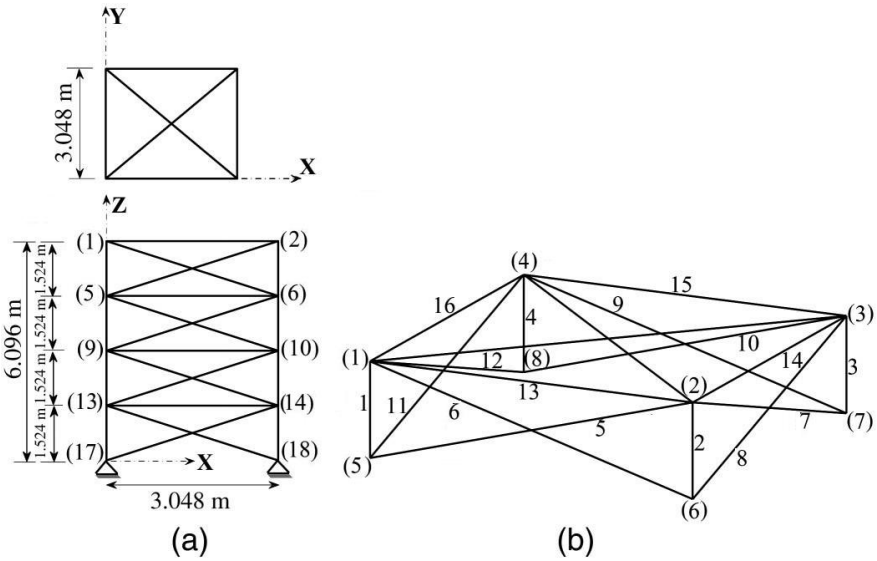

Figure 1. Schematic of the 72-bar spatial truss

Table 1: Comparison of the results obtained using the EVPS algorithm for different α and β for the 72-bar spatial truss

Element Group		Optimal cross-sectional areas (in^2)					
		α=1;β=0	α=1;β=0.1	α=1;β=0.2	α=1;β=0.3	α=1;β=0.4	α=1;β=0.5
1	A1-A4	0.156382336	0.512106532	1.309332008	0.908425451	1.874540491	1.623065446
2	A5-A12	0.538465835	0.702245646	0.709756161	0.757352394	0.700835148	1.109471213
3	A13-A16	0.409686631	0.569825371	0.344615959	0.497998885	0.705228146	0.418962252
4	A17-A18	0.576270936	0.654444669	0.795257430	0.566873163	0.593936322	1.205744400
5	A19-A22	0.541714558	0.461702274	0.496933748	1.259719082	0.642599636	1.180822331
6	A23-A30	0.518126842	0.515782142	0.653255329	0.640885800	0.697247113	0.888463363
7	A31-A34	0.100145168	0.187898838	0.132255950	0.225867449	0.203053223	0.556695994
8	A35-A36	0.102084773	0.231003396	0.154757656	0.453195412	0.265299434	0.191183802
9	A37-A40	1.267119562	0.968276468	1.422030752	1.527111585	2.440956168	1.988193574
10	A41-A48	0.505077849	0.525019151	0.549883623	0.918076745	0.750552029	0.956995112
11	A49-A52	0.100628195	0.142261126	0.194959426	0.289379054	0.286201008	0.439514823
12	A53-A54	0.100268924	0.149572223	0.161942750	0.302606930	0.352873102	0.258416359
13	A55-A58	1.893785728	2.025659715	1.992752720	2.713430340	3.333570610	3.122304105
14	A59-A66	0.517756985	0.487941757	0.534716714	0.410331980	0.766471108	0.778318545
15	A67-A70	0.100353885	0.163037131	0.384439768	0.249126698	0.274050805	0.241665049
16	A71-A72	0.100224224	0.176892391	0.210415059	0.674901952	0.286457923	0.299924469
Best weight (lb)		379.7518	426.8395	483.5943	574.8568	633.2346	736.5318
	SDS_x	0.0131	0.00931	0.00901	0.00799	0.00733	0.006077
	SDS_y	0.0131	0.00948	0.00926	0.00826	0.00770	0.005880
	SDS_z	0.0058	0.00173	0.00111	0.00103	0.00079	0.000744

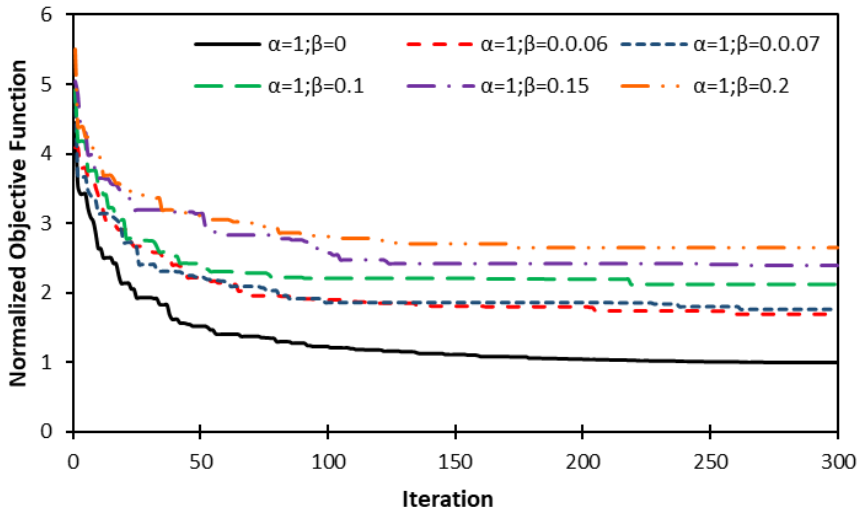

Figure 2. The convergence curves for the spatial 72-bar spatial truss based on different values of α and β

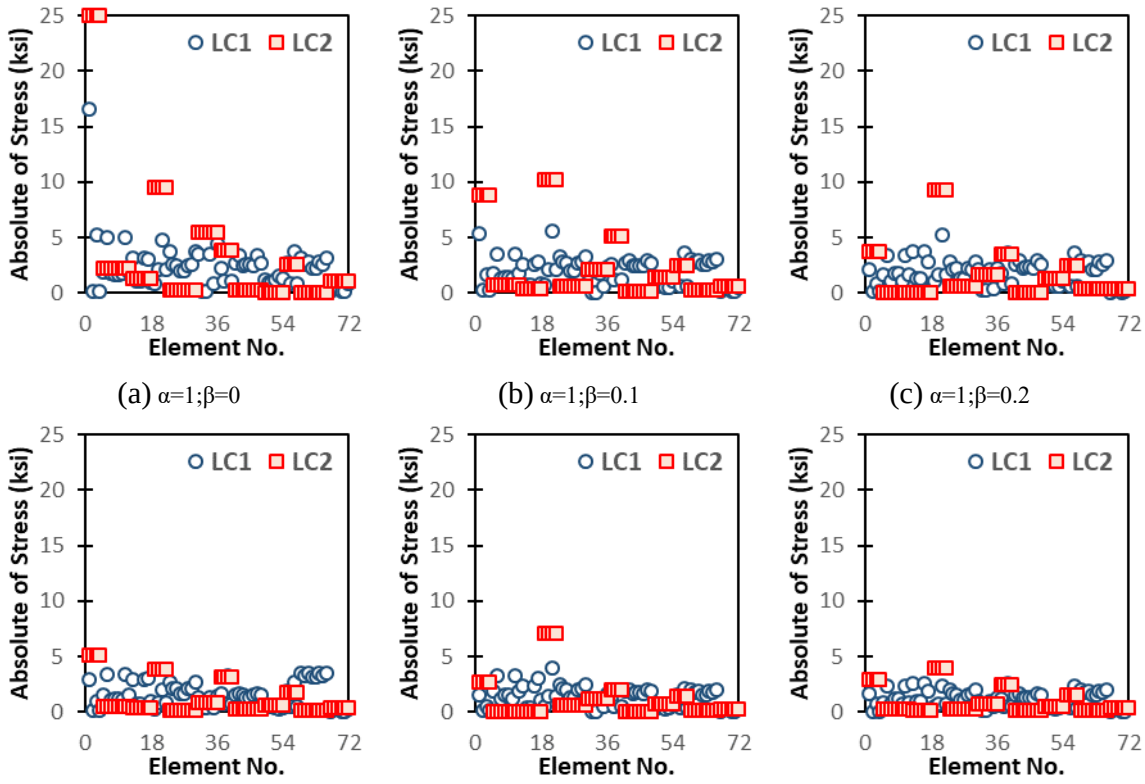

(a) α=1;β=0 (b) α=1;β=0.1 (c) α=1;β=0.2

(d) α=1;β=0.3 (e) α=1;β=0.4 (f) α=1;β=0.5

Figure 3. Comparing the absolute stress limitation obtained with the EVPS algorithm for different α and β for the 72-bar spatial truss

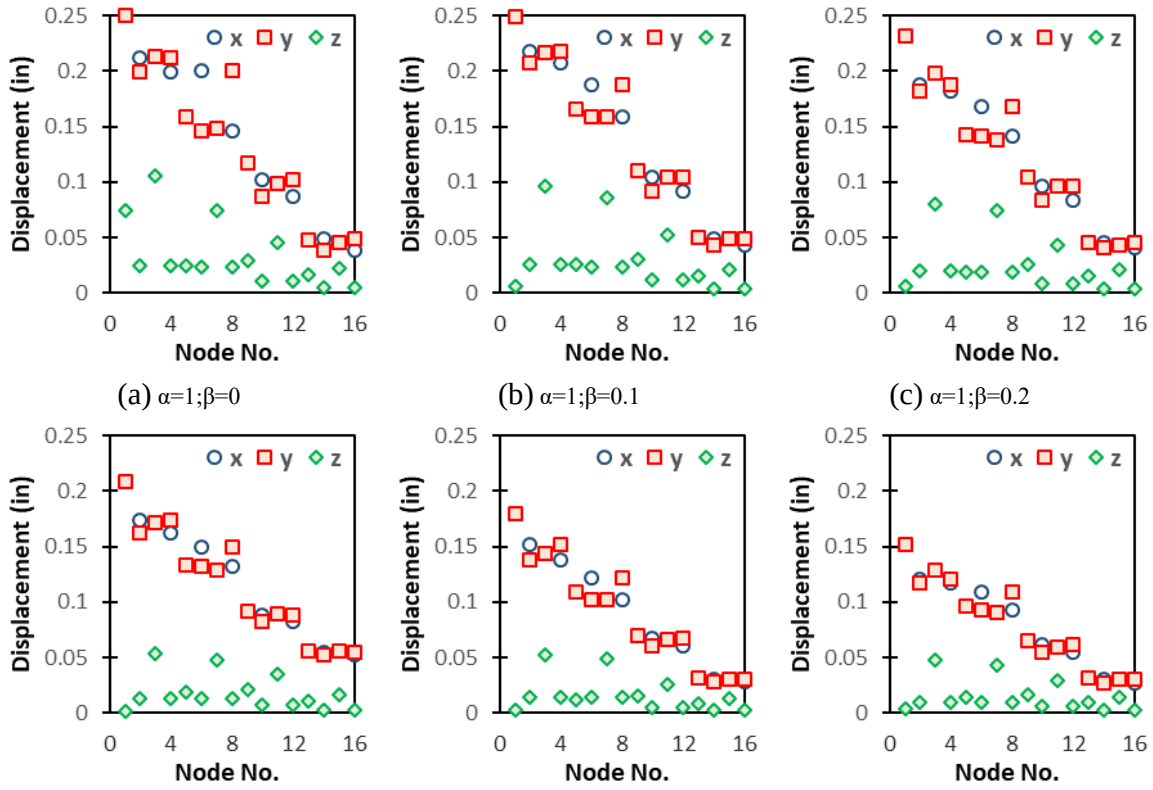

(a) α=1;β=0 (b) α=1;β=0.1 (c) α=1;β=0.2

(d) α=1;β=0.3 (e) α=1;β=0.4 (f) α=1;β=0.5

Figure 4. Comparison of the displacement limitation obtained using the EVPS algorithm for different types of α and β in x-,y-,z-direction for the 72-bar spatial truss for LC1.

4.1 A 582-bar tower truss

As shown in FIg. 5, the schematic for the 582-bar tower truss with a height of 80 m is shown. According to the symmetry of the tower, the 582 members are divided into 32 independent size variables based on their positions around the x-axis and y-axis.

The single load case is considered to consist of lateral loads of 5.0 kN applied in both x and y directions and a vertical load of -30 kN applied in the z-direction at all tower nodes. To size the variables, a discrete set of 137 economical standard steel sections is selected from a list of W-shaped profiles based on the area and radii of gyration. 39.74 cm2 and 1387.09 cm2 are taken as the lower and upper bounds of size variables. According to ASD-AISC [30], members are subject to stress and displacement limitations. Also, nodal displacements should not exceed 8.0 cm or 3.15 in. in any direction. Additionally, the maximum slenderness ratio for tension members is limited to 300, and for compression members it is recommended to be 200 in accordance with ASD-AISC design code provisions [30].

Table 2 presents the results for the optimal design obtained by using the weight part of Eq. (1) along with the effect of both parts of Eq. (1). Additionally, the results are compared with the different coefficients of α and β. According to Table 2, with an increase in the β coefficient, the weight of the structure and the robustness index will increase. According to

Eq. (4), the objective function is considered in this example based on the conditions of the problem.

$$Objective\ function = \alpha \frac{WS\{x\}}{21.33} + \frac{\beta}{3}\left[\frac{SDS_x\{x\}}{0.00033} + \frac{SDS_y\{x\}}{0.00033} + \frac{SDS_z\{x\}}{0.0000471}\right] \quad (4)$$

where, according to the first loading, SDS_x, SDS_y and SDS_z correspond to displacement of the node at the highest level in the x, y, and z directions.

Based on different values of α and β, FIg. 6 illustrates the convergence curves for the 582-bar spatial truss. As shown in FIg. 7, ratio of demand to capacity (D/C) obtained using the EVPS algorithm for different α and β for the 582-bar spatial truss is compared, while FIg. 8 illustrates a comparison of the displacement limitations in 3 directions obtained by using the EVPS algorithm for different types of α and β for the 582-bar spatial truss.

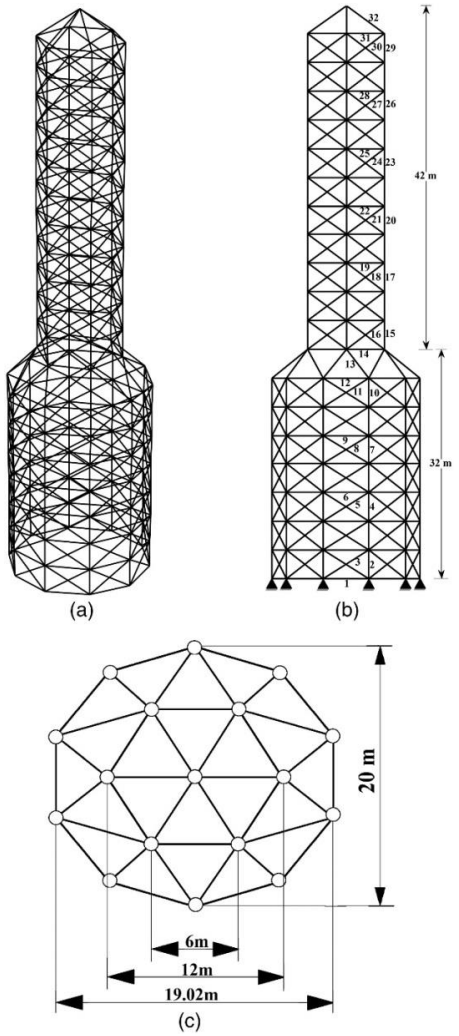

Figure 5. Schematic of the 582-bar tower truss

Table 2: Comparison of the results obtained using the EVPS algorithm for different α and β for the 582-bar spatial truss

Element Group	Optimal cross-sectional areas (cm^2)					
	α=1;β=0	α=1;β=0.06	α=1;β=0.07	α=1;β=0.1	α=1;β=0.15	α=1;β=0.2
1	39.741856	58.903108	39.741856	47.354744	45.677328	72.257920
2	146.45132	123.22556	146.45132	192.25768	231.61244	278.70912
3	45.677328	57.096660	49.354740	64.516000	45.677328	53.225700
4	114.19332	115.48364	149.67712	278.70912	221.93504	250.32208
5	47.354744	53.225700	49.354740	58.903108	84.515960	66.451480
6	39.741856	39.741856	92.903040	85.806280	64.516000	41.870884
7	94.193360	92.903040	75.483720	136.12876	249.03176	189.67704
8	47.354744	47.354744	45.677328	58.903108	53.225700	49.354740
9	41.870884	47.354744	41.870884	45.677328	45.677328	66.451480
10	75.483720	126.45136	249.03176	64.516000	165.16096	250.32208
11	45.677328	64.516000	58.903108	57.096660	45.677328	62.645036
12	146.45132	285.80588	187.74156	447.74104	226.45116	231.61244
13	136.12876	128.38684	149.67712	206.45120	169.03192	334.19288
14	94.193360	92.903040	114.19332	100.64496	115.48364	167.74160
15	167.74160	123.22556	118.06428	338.70900	379.35408	334.19288
16	47.354744	45.677328	45.677328	81.290160	66.451480	58.903108
17	115.48364	115.48364	198.06412	226.45116	328.38644	277.41880
18	47.354744	47.354744	57.096660	64.516000	49.354740	58.903108
19	39.741856	53.225700	47.354744	74.193400	118.06428	49.354740
20	84.515960	75.483720	221.93504	94.193360	126.45136	183.87060
21	45.677328	57.096660	62.645036	49.354740	49.354740	64.516000
22	39.741856	45.677328	58.903108	140.64488	41.870884	45.677328
23	45.677328	159.35452	85.806280	123.22556	216.77376	167.74160
24	47.354744	49.354740	47.354744	56.709564	49.354740	75.483720
25	41.870884	41.870884	41.870884	66.451480	85.806280	189.67704
26	47.354744	72.257920	92.903040	62.645036	114.19332	81.290160
27	45.677328	64.516000	47.354744	64.516000	58.903108	66.451480
28	41.870884	81.290160	72.257920	49.354740	84.515960	128.38684
29	41.870884	136.12876	187.74156	178.06416	165.16096	136.12876
30	45.677328	53.225700	47.354744	68.386960	47.354744	49.354740
31	39.741856	84.515960	94.193360	84.515960	277.41880	62.645036
32	45.677328	114.19332	57.096660	53.225700	136.12876	75.483720
Best weight (m^3)	21.33374	25.43614	26.46044	33.35603	34.11437	37.05126
SDSx	0.004073	0.002921719	0.002645702	0.001924	0.001879	0.00158686
SDSy	0.003844	0.002677016	0.002490255	0.001824	0.001777	0.00150095
SDSz	0.000586	0.000372407	0.000337201	0.000264	0.000229	0.000208790

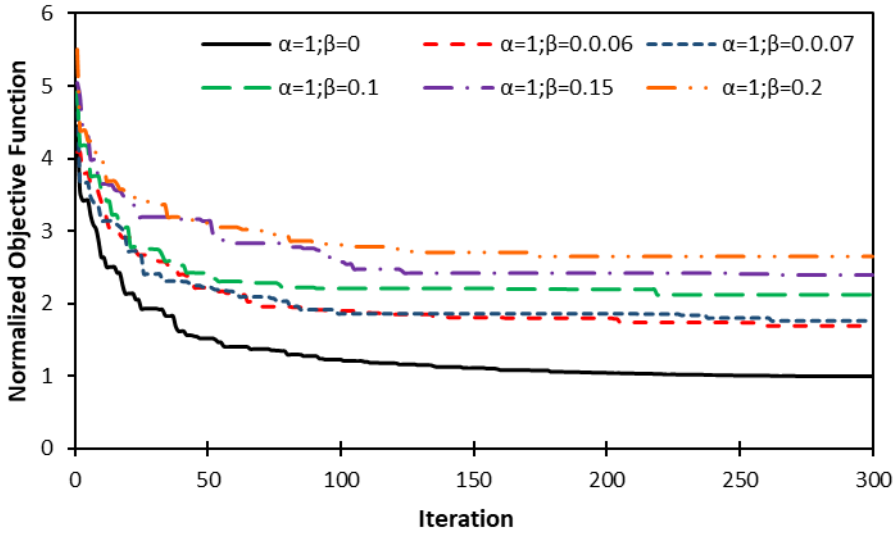

Figure 6. The convergence curves for the spatial 582-bar spatial truss based on different values of α and β

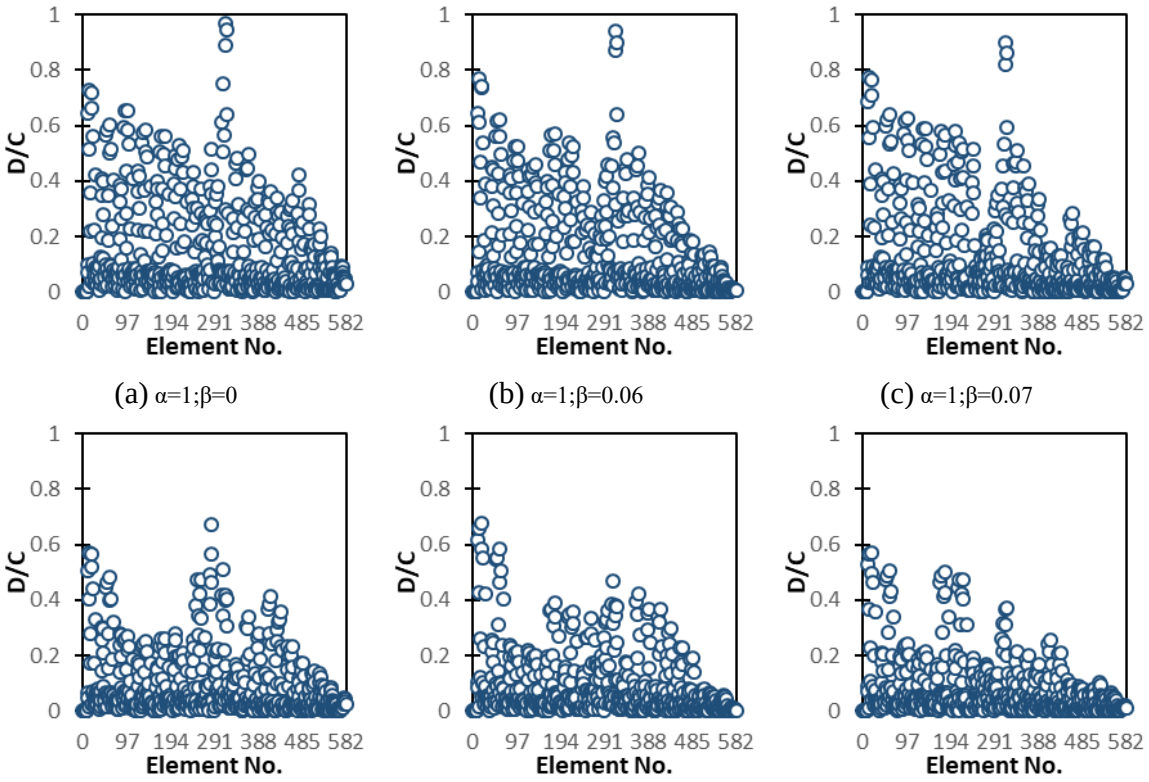

(a) α=1;β=0 (b) α=1;β=0.06 (c) α=1;β=0.07

(d) α=1;β=0.1 (e) α=1;β=0.15 (f) α=1;β=0.2

Figure 7. Comparing the deman-to-capacity ratio limitation obtained with the EVPS algorithm for different α and β for the 582-bar spatial truss

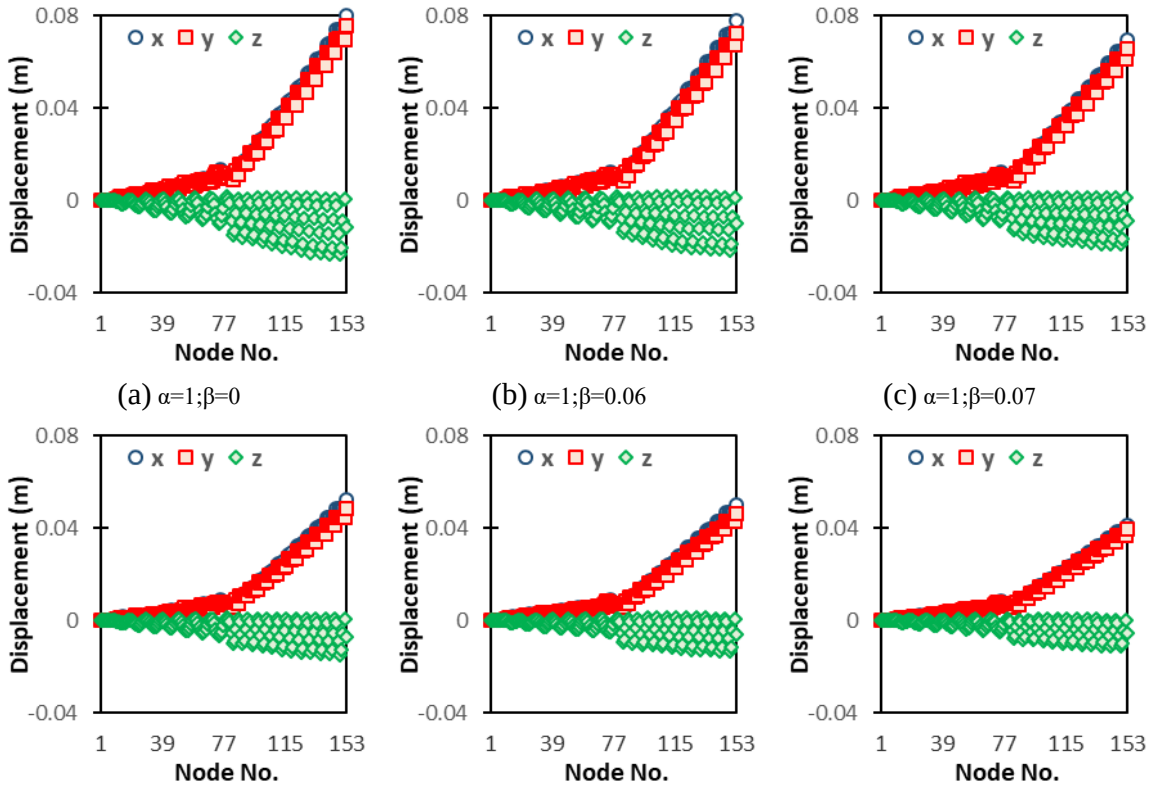

(a) α=1;β=0 (b) α=1;β=0.06 (c) α=1;β=0.07

(d) α=1;β=0.1 (e) α=1;β=0.15 (f) α=1;β=0.2

Figure 8. Comparison of the displacement limitation obtained using the EVPS algorithm for different types of α and β in x-,y-,z-direction for the 582-bar spatial truss.

5. CONCLUSION

This study examines the optimal robust design for three-dimensional trusses. A robust design optimization objective function, consisting of two parts: a weight and a robustness index, has been considered for this purpose. The robustness of the response is assumed on one node of each truss in all three directions. Two steel space trusses were optimized based on uncertainties associated with the modulus of elasticity, yield stress, and cross-sections. Parameters with uncertainty are considered random variables with statistical distributions. Modeling uncertainties uses a normal probability distribution of random variables. In this study, the effect of various robustness index coefficients (β) of the objective function was examined, and the results indicated that with the increase of this coefficient, the robustness index will decrease and the weight will increase. According to the results, as the robustness index coeficient (β) increases, the considered limits have moved away from the allowable limits toward a safe margin. As a result of the obtained results, it can be concluded that the objective function has achieved the intended outcome.

REFERENCES

1. Kennedy J, Eberhart R. Particle swarm optimization. in: neural networks, *Proceedings of IEEE International conference on neural networks*; pp. 1942-1948.
2. Qin AK, Huang VL, Suganthan PN. Differential evolution algorithm with strategy adaptation for global numerical optimization, *IEEE Transact Evolut Computat* 2008; **13**(2): 398-417.
3. Jalili S, Kashan AH, Hosseinzadeh Y. League championship algorithms for optimum design of pin-jointed structures, *J Comput Civil Eng* 2016; **31**(2): 04016048.
4. Shabani A, Asgarian B, Salido M, Gharebaghi SA. Search and rescue optimization algorithm: A new optimization method for solving constrained engineering optimization problems, *Expert Syst Applicat* 2020; **161**: 113698.
5. Rao RV, Savsani VJ, Vakharia D. Teaching–learning-based optimization: a novel method for constrained mechanical design optimization problems, *Comput-Aid Des* 2011; **43**(3): 303-15.
6. Mirjalili S, Mirjalili SM, Lewis A. Grey wolf optimizer, *Adv Eng Softw* 2014; **69**: 46-61.
7. Kaveh A, Hosseini P. A simplified dolphin echolocation optimization method for optimum design of trusses, *Int J Optim Civil Eng* 2014; **4**(3): 381-97.
8. Kaveh A, Hoseini Vaez SR, Hosseini P, Fallar, N. Detection of damage in truss structures using Simplified Dolphin Echolocation algorithm based on modal dat, *Smart Struct Syst* 2016; **18**(5): 983-1004.
9. Kaveh A, Hoseini Vaez SR, Hosseini P. Simplified dolphin echolocation algorithm for optimum design of fram, *Smart Struct Syst* 2018; **21**(3): 321-33.
10. Kaur A, Kumar Y. A new metaheuristic algorithm based on water wave optimization for data clusterin, *Evolut Intell* 2021; **15**(1): 759-83.
11. Hashim FA, Houssein EH, Hussain K, Mabrouk MS, AlAtabany W. Honey Badger Algorithm: New metaheuristic algorithm for solving optimization problems, *Math Comput Simul* 2022; **192**: 84-110.
12. Calafiore GC, Dabbene F. Optimization under uncertainty with applications to design of truss structure, *Struct Multidiscip Optim* 2008; **35**(3): 189-200.
13. Asadpoure A, Tootkaboni M, Guest JK. Robust topology optimization of structures with uncertainties in stiffness – Application to truss structures, *Comput Struct* 2011; **89**(11): 1131-41.
14. Kang Z, Bai S. On robust design optimization of truss structures with bounded uncertaintie, *Struct Multidisc Optim* 2013; **47**(5): 699-714.
15. Richardson JN, Rajan FC, Adriaenssens S. Robust topology optimization of truss structures with random loading and material properties: A multiobjective perspective, *Comput Struct* 2015; **154**: 41-7.
16. Assimi H, Jamali A, Narimanzadeh N. Multi-objective sizing and topology optimization of truss structures using genetic programming based on a new adaptive mutant operator, *Neural Comput Appl* 2019; **31**(10): 5729-49.
17. Kaveh A, Hoseini Vaez SR, Hosseini P, Fatali MA. Heuristic Operator for Reliability Assessment of Frame Structures, *Period Polytech Civil Eng* 2021; **65**(3): 702-16.
18. Hoseini Vaez SR, Hosseini P, Fatali MA, Asaad Samani A, Kaveh A. Size and shape reliability-based optimization of dome trusses, *Int J Optim Civil Eng 2020;* **10**(4): 701-14.

19. Hosseini P, Kaveh A, Hatami N, Hoseini Vaez SR. The optimization of large-scale dome trusses on the basis of the probability of failure. *Int I Optim Civl Eng* 2022; **12**(3): 457-75.
20. Hosseini P, Hoseini Vaez SR, Fatali MA, Mehanpour H. Reliability assessment of transmission line towers using metaheuristic algorithms, *Int J Optim Civil Eng* 2020; **10**(3): 531-51.
21. Hoseini Vaez SRAsaad Samani A, Mobinipour SA, Dehghani, E. Effect of Uncertainties in Design Variables on the Hysteresis Response of 2D Steel Moment-Resisting Frames, *Practice Period Struct Des Construct* 2022; **27**(4): 04022044.
22. Kaveh A, Rahami H. Analysis, design and optimization of structures using force method and genetic algorithm, *Int J Numer Meth Eng* 2006; **65**(10): 1570-84.
23. Kaveh A, Malakoutirad S. Hybrid genetic algorithm and particle swarm optimization for the force method-based simultaneous analysis and design, *Iranian J Sci Technol Transact B - Eng* 2010; **34**: 15-34.
24. Kaveh A, Hoseini Vaez SR, Hosseini P. Enhanced vibrating particles system algorithm for damage identification of truss structures, *Scientia Iranica* 2019; **26**(1): 246-56.
25. Kaveh A, Talatahari S A charged system search with a fly to boundary method for discrete optimum design of truss structures, *Asian J Civil Eng (Building and Housing)* 2010; **11**(3): 277-93.
26. Kaveh A, Hoseini Vaez SR, Hosseini P, Fatali MA. A new two-phase method for damage detection in skeletal structures, *Iranian J Sci Technol, Transact Civil Eng* 2019; **43**(1): 49-65.
27. Kaveh A, Hoseini Vaez SR, Hosseini P. Performance of the modified dolphin monitoring operator for weight optimization of skeletal structures, *Period Polytech Civil Eng* 2019; **63**(1): 30-45.
28. Kaveh A, Javadi SM, Shape and size optimization of trusses with multiple frequency constraints using harmony search and ray optimizer for enhancing the particle swarm optimization algorithm, *Acta Mech* 2014; **225**(6): 1595-605.
29. Kaveh A, Hosseini P, Hatami N, Hoseini Vaez SR. Large-scale dome truss optimization with frequency constraints using EVPS algorithm, *Int J Optim Civil Eng* 2022; **12**(1): 105-23.
30. Kaveh, A., S. Hoseini Vaez, and P. Hosseini, MATLAB code for an enhanced vibrating particles system algorithm, *Int J Optim Civil Eng* 2018; **8**(3): 401-14.
31. Baker JW, Schubert M, Faber MH. On the assessment of robustness, *Struct Safe* 2008; **30**(3): 253-67.
32. Kim SE, Truong VH. Reliability evaluation of semirigid steel frames using advanced analysis, *J Struct Eng* 2020; **146**(5): 04020064.